CMLS, Cell. Mol. Life Sci. 62 (2005) 471–484
1420-682X/05/040471-14
DOI 10.1007/s00018-004-4423-2

CMLS Cellular and Molecular Life Sciences

Research Article

Association, mutual stabilization, and transcriptional activity of the STRA13 and MSP58 proteins

A. V. Ivanova [a,*], S. V. Ivanov [a] and M. L. Lerman [b]

[a] Laboratory of Immunobiology, Basic Research Program, SAIC-Frederick Inc., NCI-Frederick, Maryland 21702 (USA), Fax: +1 301 846 6145, e-mail: ivanova@mail.ncifcrf.gov
[b] Laboratory of Immunobiology, NCI-Frederick, Maryland 21702 (USA)

Received 22 September 2004; received after revision 7 December 2004; accepted 17 December 2004

Abstract. STRA13 is a hypoxia-inducible bHLH transcription factor implicated in the pVHL/HIF, TGF-beta, and Jak/STAT pathways. To further characterize the STRA13 protein-interacting network and mechanisms of STRA13-dependent transcription, we utilized yeast two-hybrid screening. Here we report on STRA13 interaction with the cell cycle-associated transcription factor MSP58. We demonstrated that the basic domain of STRA13 and the FHA domain of MSP58 are essential for this association. We performed phospho-peptide mapping of both MSP58 and STRA13 and showed that their association was modulated by the STRA13 phosphorylation status. STRA13/MSP58 complex formation protected both proteins from the proteasome-mediated degradation, extending their half-lives considerably. STRA13 and MSP58 synergistically co-operated in the STRA13 promoter-driven transcription repression. Both proteins were co-localized in the nucleus and showed transcript accumulation during the S phase of the cell cycle. Thus, we characterize a novel STRA13-associated transcription repression complex and provide a link between cell cycle regulation and STRA13 activity.

Key words. STRA13; MSP58; bHLH domain; FHA domain; mutual stabilization; phosphorylation; synergistic repression; cell cycle.

STRA13 is a nuclear bHLH-type transcriptional factor regulated by the pVHL tumor suppressor and over-expressed in cancers of the brain, lung, and kidney [1, 2]. Its broad-range expression in embryonic and adult tissues combined with responsiveness to various stimuli, including hypoxia [2, 3], cytokines [4, 5], retinoic acid [6], cAMP [7], serum deprivation, a histone deacetylase inhibitor trichostatin A [8], gonadotropins [9], and insulin [10] imply important roles for STRA13 in multiple signal transduction pathways and various biological processes from regulation of cell metabolism to morphogenesis. Indeed, this transcription factor has been implicated in neurogenesis [6], adipogenesis [11], chondrogenesis [12], and regulation of mammalian circadian rhythms [13, 14]. Studies on mouse knockout and transgenic models highlighted a crucial role for STRA13 in regulation of early B and T cell development, late B cell activation, and terminal differentiation [15, 16]. While STRA13 biochemical functions were associated with growth suppression [8] and regulation of apoptosis [5, 15], the molecular mechanisms of its action are still unclear and need further investigation. STRA13 transcriptional activity was associated with general transcriptional factors, such as TBP and TFIIB [6], with a bHLHZip factor USF [17], and with signal transducer and activator of transcription 3 (STAT3) [5].

Here we report on the physical and functional interaction between STRA13 and MSP58. The MSP58 protein (also known as P78 and MCRS1) possesses an FHA (forkhead-associated) domain and is implicated in regulation of pro-

* Corresponding author.

liferation and apoptosis as a part of the transcriptional repressor complex with p120 and Daxx [18, 19]. It was also found to be tightly regulated in the cell cycle, accumulating in the very early stage of the S phase [20]. A study of the quail homologue of MSP58, TOJ3, showed that this protein can be up-regulated by v-Jun and that TOJ3 overexpression induces cell transformation [21]. A splice isoform of human MSP58, MCRS2, which is 13 N-terminal amino acids longer then MSP58, was found to interact and cytologically co-localize with a putative tumor suppressor and a potent telomerase inhibitor LPTS/PinX1, and hTERT, the catalytic telomerase subunit [22]. Forced expression of MCRS2 inhibited telomerase in vitro and resulted over time in a gradual and progressive shortening of telomeres, suggesting that MCRS2 provides a link between the cell cycle and telomere length regulation.

To further investigate STRA13 involvement in carcinogenesis, we applied yeast two-hybrid system to search for new protein partners that may be involved in cell cycle progression. We found that STRA13 binds to the cell cycle-dependent transcription factor MSP58/MCRS1. We further demonstrated that co-expression of STRA13 and MSP58 stabilized both proteins, markedly increasing their half-life. We showed that MSP58 is subject to 26S proteasome degradation and suggest that formation of the MSP58/STRA13 complex possibly prevents interaction with the proteasome machinery. These results combined with co-localization of both partners in the nucleus and an overlap in their expression during cell cycle suggest that STRA13 and MCP58 can be recruited as parts of the same transcription complex(s). Finally, we demonstrate that co-expression of both proteins results in synergistic repression of the STRA13-luc promoter, which was previously shown to be STRA13 dependent [8].

Materials and methods

Yeast two-hybrid screen

The entire open reading frame of the STRA13 (411 amino acid residues) was inserted into *Eco*RI-*Bam*HI restriction site of the pAS2-1 expression vector (Clontech) that was used as a bait. Two-hybrid screening was performed as described in our previous paper [2] using Clontech Matchmaker human kidney cDNA library.

Plasmid constructs

STRA13 and a series of its deletion mutants were generated by amplification of the fragments from the human cDNA and cloned into the *Eco*RI-*Xba*I site of the pCMV2-FLAG vector. The constructs have been verified by sequencing. The MSP58-HA plasmid for confirmation of interaction with STRA13 was generated by subcloning of the 1.6-kb *Eco*RI-*Xho*I insert from the pACT2 plasmid obtained by screening of the fetal kidney cDNA Matchmaker cDNA library (Clontech) for STRA13 interactors. The full-length isoforms of MSP58 in the pCMV-HA plasmid were generated as described in Results. The luciferase reporter driven by a 1.1 kb fragment of the human STRA13 promoter was generated by introduction of the PCR product obtained on human DNA (pos. 3405–4533, region 4956968–4971101 of the human chromosome 3 contig, accession no. NT_022517) into the *Kpn*I/*Bgl*II site of the pTA-luc vector (BD Biosciences). The resulting construct was verified by sequencing.

Cell culture

HEK 293T cells are a human embryonic kidney cell line [American Type Culture Collection (ATCC)]; COS-7 cells are an SV40-transformed African green monkey kidney cell line (ATCC). Cell lines transfected with VHL constructs are described in Ivanov et al. [1]. Cell lines were maintained in DMEM (GIBCO BRL) supplemented with 0.1% penicillin-streptomycin (Sigma-Aldrich) and 10% FBS. Cells were maintained/ incubated at 37 °C in 5% CO_2.

RT-PCR

Total RNA was prepared from cells using RNeasy mini Kit (Qiagen). The quantity of RNA was assessed by spectrophotometer. RT-PCR reactions were performed using the SuperScript One-step RT-PCR Kit (Invitrogen). The PCR reaction protocol was as follows: 25 cycles (denaturation at 94 °C for 30 s, annealing at 55 °C for 30 s, and extension at 72 °C for 1 min). This number of cycles was previously determined to be optimal for detecting the signal in a linear range. The QuantumRNA Classic II 18S Internal Standard kit (Ambion) was used to provide an internal control for the quantitative RNA analysis. Amplification products were visualized, photographed and quantified using the Kodak Image Station 2000RT.

Immunoprecipitations and immunoblotting

Sub-confluent 293T cells were transfected with 5 µg DNA with the lipofectamin^{2000} reagent (Invitrogen) in a 10-cm dish. Twenty-four or 48 h later, cells were harvested and lysed in RIPA buffer [150 mM NaCl, 50 mM Hepes (pH 7.4), 10 mM NaF, 1 mM EDTA, 2 mM orthovanadate, 10% glycerol, 1% Triton, 1% deoxycholate, 0.5% SDS, protease inhibitors], the lysates were sheared by ultrasound and cleared by centrifugation at 13,000 rpm for 15 min at 4 °C. Cell lysates containing an equal amount of total protein were incubated for 4 h at 4 °C with 50 µl of 30% protein G-sepharose beads (Stratagene) and anti-FLAG monoclonal antibody or control (IgG) antibodies. The beads were washed extensively with lysis buffer and bound proteins were fractionated on 8–16% SDS-PAGE, transferred to a nitrocellulose membrane, and incubated with the anti-HA antibodies. Flag- or HA-fused proteins were visualized using the ECL kit (DURA; Pierce).

Synchronization of 293T cells

Double-thymidine block was used to synchronize the cell cycle. 293T cells were first treated with 20 mM thymidine in DMEM for 20 h at 37 °C in 5% CO_2. Cells were then washed with Tris-saline and incubated in fresh medium for 7 h. 20 mM thymydine was then added for the second thymidine block, and cells were incubated for 17 h. The final Tris-saline wash and incubation in fresh medium was followed by the beginning of time points, as cells exit simultaneously from G1/S of the cell cycle

Transient transfection and luciferase reporter assay

For transient transfection, 293T cells were grown in six-well plates to 70–80% confluence and co-transfected with the indicated reporter constructs and 1.0 µg of the plasmids containing STRA13 (or its mutants) and (or) MSP58 (or its mutants) using lipofectamin™ 2000 reagent (Stratagene). Forty-eight hours post-transfection luciferase activity was detected by mixing 20 µl of the lysate with 100 µl of luciferase substrate (Promega) and measured in a MicroLumat LB96P luminometer (EG&G Berthold). The luciferase activity was normalized based on protein concentration. Fold induction was calculated by dividing the treated samples by the nontreated control for each reporter construct. Mean and standard deviation were calculated based on five independent experiments.

Immunostaining

293T or COS-7 cells were transiently transfected with various STRA13/FLAG or (and) MSP58/HA constructs. Twenty-four hours post-transfection, cells were cultured on coverslips overnight, washed in PBS, fixed in 4–7% paraformaldehyde for 30 min, and permeabilized with 0.1% Triton X-100 for 5 min. After pre-incubation with 1% fetal bovine serum, cells were immunostained with anti-FLAG M2 mouse monoclonal antibodies. Goat anti-mouse antibodies with Alexa Fluor 488 (green) were used to visualize the anti-FLAG mouse monoclonal antibody. Cells immunostained with anti-HA rat antibodies (Roche) were visualized with Alexa Fluor TM 594 (red) anti-rat antibodies.

Phosphatase inhibitor treatment

293T cells were co-transfected with STRA13 and MSP58, replated 24 h later and treated for 30 min with 100 nM of the serine/threonine phosphatase inhibitor calyculin A (Cell Signaling) or 100 µM of the tyrosine phosphatase inhibitor sodium orthovanadate 18 h later.

Results

STRA13 interacts with MSP58 in yeast cells

The yeast two-hybrid protein interaction screening was carried out to isolate cellular protein(s) capable of binding to the full-length STRA13 protein. The yeast strain CG1945 was simultaneously transformed with a 'bait' plasmid expressing the STRA13 open reading frame and human kidney cDNA library. Transformants (approximately 2×10^6) were subjected to dual a selection (HIS+, LacZ+) and the nucleotide sequences of positive clones were determined. One of the selected clones encoded almost entire MSP58 (MCRS1) protein (residues 31–462) lacking 30 amino acids from its N terminus. A retransformation assay showed that the GAL4-AD-MSP58 fusion protein interacted with STRA13 specifically, since no binding of AD-MSP58 was detected with either the pAS2-1 vector alone (the binding domain, BD) or with pAS2-1-ARNT1 that produces the BD-ARNT1 fusion protein (data not shown). From these experiments we concluded that the STRA13/MSP58 interaction was specific in the yeast two-hybrid system.

Three MSP58/MCRS1 isoforms isolated from human lung and prostate transcriptomes

To obtain the full-length open reading frame of MSP58 for cloning in the mammalian vector, we performed PCR with primers that were designed based on sequence information available from GenBank (NM_006337, primer positions 141–160 and 1579–1560). PCR amplification on lung and prostate cDNA libraries produced three bands of different intensities. Cloning and sequencing showed that these bands corresponded to at least three splice isoforms of MSP58 (fig. 1A, upper panel). An in silico study showed that there are three ATG initiating codons and one termination codon that may be potentially used for protein translation. Three putative open reading frames of 462 (isoform A, initiating ATG at pos. 192, NM_006337), 475 (isoform B, ATG at pos. 534, AF068007), and 449 amino acids (isoform C, ATG at pos. 231, NM_006337) were identified (fig. 1A, upper panel). Isoform A was found to have a 509-bp deletion in 3′ close proximity to the ATG (192) codon, while isoform B showed a 178-bp deletion 3′ adjacent to its initiating ATG codon (fig. 1A, upper panel). The longest isoform C appeared to be the only one that contained two potential open reading frames. However, a stop codon found in-frame with the most 5′ ATG rendered the hypothetical polypeptide negligibly small. The other open reading frame possessed an initiating ATG codon at position 231 and encoded a 449-amino acid hypothetical protein.

Despite this cDNA variability, polypeptide sequences deduced for all three isoforms appeared to be mostly identical, differing only by a short N-terminal extension (fig. 1A, lower panel). Each of these three cDNAs has already been characterized elsewhere [18, 20, 22]. However, during our sequencing analysis, we came to the conclusion that cDNA for the p78 protein reported by Bruni at al. [20], accession no. AF068007, contained several errors

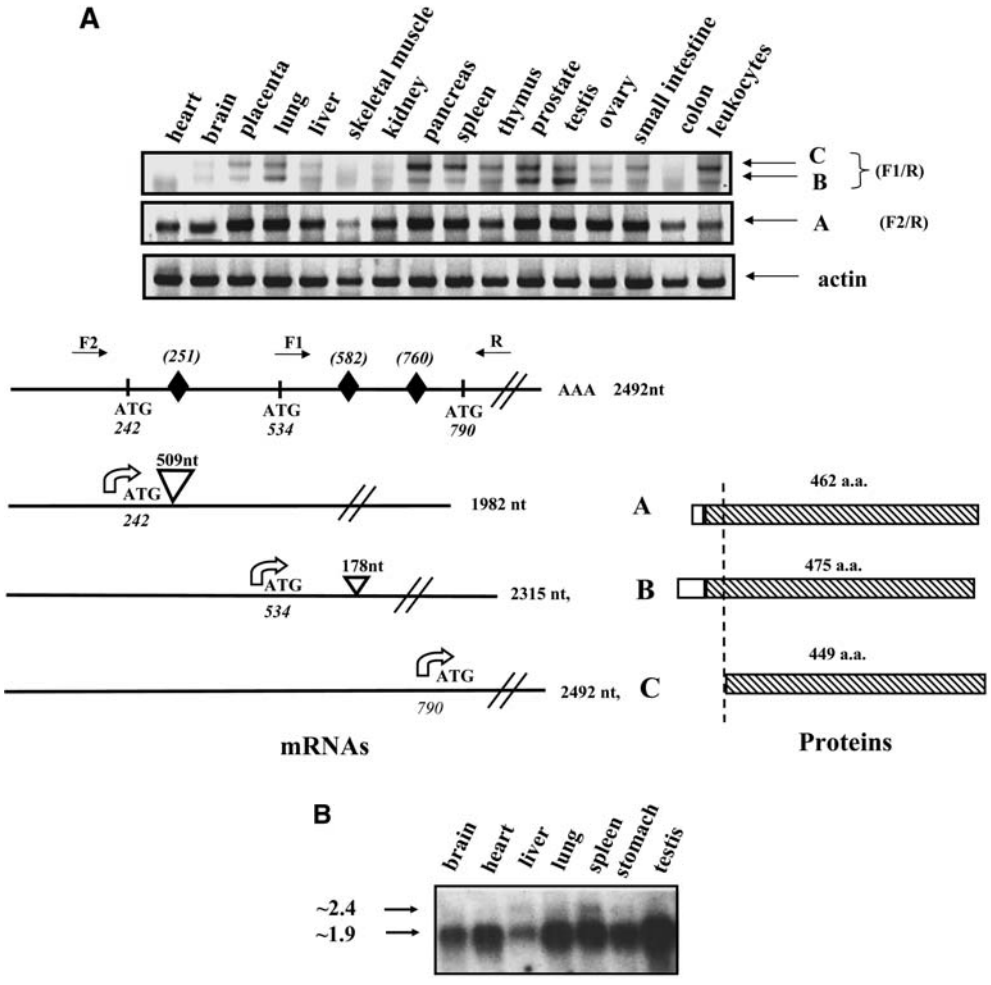

Figure 1. Three differentially spliced MSP58 mRNA isoforms. (*A*) Upper panel: PCR on cDNA extracted from different tissues (MTN cDNA panel; Clontech) shows distribution of MSP58 mRNA in human tissues. Primers F1 and R produce two low-intensity bands consistent with isoforms B (178 bp spliced out) and C (nonspliced isoform), primers F2 and R produce one major band that is characteristic for the A isoform (509 bp spliced out). Bottom panel: a schematic presentation of MSP58 mRNA isoforms. The longest cDNA is shown at the top and the bottom of the picture. Positions of predicted ATG initiation codons are shown with vertical bars. Three large black diamonds show positions of the sites for splicing out 509 bp (variant A) or 178 bp (variant B). Predicted protein sequences for all three isoforms are shown on the right. Hatched boxes show common protein segments. (*B*) MSP58 expression in human tissues. Northern Light Blot (Panomics) was used to perform Northern Blot analysis. The film was intentionally overexposed to reveal upper bands of the nonspliced form of the MSP58 mRNA. Two MSP58 bands that differ by approximately 500 nucleotides are indicated by arrows. Molecular sizes are shown in kilobases.

translated into an incorrect N-terminal protein sequence. A similar conclusion was made earlier by Song et al. [22]. To study MSP58 isoform distribution in human tissues, we designed primers and performed PCR using MTN cDNA panels from Clontech (fig. 1A, lower panel). Primers F1 and R produced two low-intensity bands consistent with isoforms B and C that differ by 178 bp. The primer set F2 and R, which was expected to generate three bands corresponding to isoforms A, B, and C, produced instead only one major band that was matched to the A isoform. Based on these data, we concluded that isoform A is the most predominant among MSP58 isoforms in all tissues analyzed. Isoforms B and C are less abundant, and show a tissue-specific distribution in some tissues (brain, skeletal muscle, kidney, and colon) displaying only negligible amounts of both transcripts. These data were complemented at the next stage by Northern analysis (fig. 1B). Examined tissues contained variable amounts of 2.4- and 1.9-kb bands. In all tissues, except for liver, the 1.9-kb band was prominent. Only liver and spleen showed visible amounts of the 2.4-kb band. Analysis of the NCBI EST database confirmed the existence of the B and C isoforms in the human transcriptome.

MSP58 and STRA13 proteins interact in mammalian cells

To confirm the MSP58/STRA13 interaction in mammalian cells, we inserted cDNA of the most abundant

MSP58 isoform A into the mammalian pCMV-HA vector to produce the HA-MSP58 fusion protein. STRA13 cDNA was fused with the FLAG tag in the pCMV2 vector. HA-MSP58 was co-transfected into 293T cells with FLAG-STRA13 or empty pCMV2 plasmid. After 48 h of incubation, STRA13 was immunoprecipitated from cell lysates with an anti-FLAG monoclonal antibody. The presence of MSP58 in STRA13 precipitates was detected using polyclonal anti-HA antibodies (fig. 2B, lane 2). The fact that MSP58 was co-precipitated with STRA13 confirms that STRA13 and MSP58 specifically interact in mammalian cells. No precipitation products were observed with the empty pFLAG-CMV2 vector (fig. 2B, lane 1).

Domain mapping studies of the STRA13/MSP58 interaction

To identify STRA13 domains that bind MSP58, a series of cDNA deletion mutants fused to the FLAG epitope in the pCMV2 plasmid (fig. 2A) and the HA-MSP58 plasmid were co-transfected into 293T cells, and proteins were co-immunoprecipitated as described above. Due to the extreme instability of STRA13 truncated proteins [2], the proteasome inhibitor ALLnL was added to the transfected cells to prevent mutants degradation. The deletion of the N-terminal part of STRA13 in the 69–412 mutant as well as further subsequent deletions of the N-terminal bHLH domain or three adjacent helices abolished the

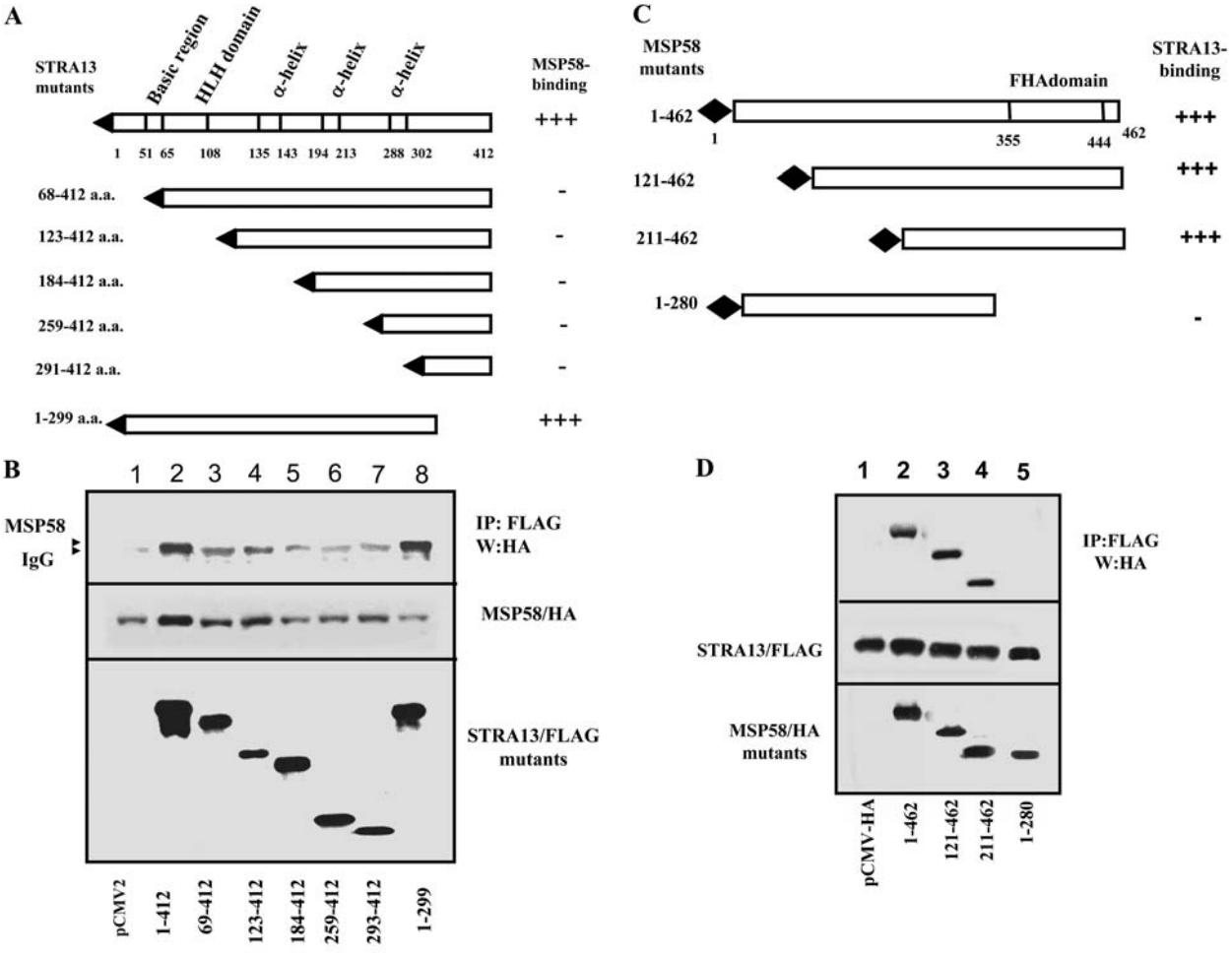

Figure 2. STRA13 and MSP58 proteins interact in mammalian cells. (*A*) Schematic representation of the STRA13 protein domain structure and its deletion mutants. STRA13 protein fragment positions are indicated on the left. All deletion mutants were fused to a FLAG-tag (black triangle) on their N termini. (*B*) STRA13 interacts with MSP58 through the STRA13 basic region. STRA13 or its mutants transiently co-transfected with the MSP58/HA construct into 293T cells were immunoprecipitated with anti-FLAG M2 antibodies (Sigma). Precipitates (IP) were analyzed by Western blotting (W). The presence of MSP58 in STRA13 mutants precipitates was detected with rat anti-HA monoclonal antibodies (Roche). The upper bands represent the IgG light chain that cross-reacted with the secondary antibody. (*C*) Schematic representation of the MSP58 domain structure and its deletion mutants. The numbers of the amino acid sequence included in the deletion constructs are indicated on the left. MSP58 protein fragment positions are indicated on the left. All deletion mutants were fused to HA-tag (black diamonds) on their N termini. (*D*) MSP58 interacts with STRA13 through the FHA (forkhead-associated) domain of MSP58. STRA13 from 293T cells transiently co-transfected with the MSP58 mutants was immunoprecipitated with anti-FLAG antibodies. Precipitates (IP) were analyzed by Western blotting (W). The presence of MSP58 mutants in STRA13 precipitates was detected with anti-HA monoclonal antibodies.

STRA13/MSP58 interaction (fig. 2B, lanes 3–7). Deletion of the C-terminal part of STRA13 in the mutant 1–299 (fig. 2B, line 8) did not lead to binding abrogation. Therefore, we defined the region between amino acid residues 1 and 68 as absolutely required for the STRA13/MSP58 interaction, and the C-terminal 299–412 region as insignificant.

To find domain(s) of MSP58 responsible for binding to STRA13, we used three MSP58 mutants fused to the HA epitope in the pCMV-HA plasmid (fig. 2C). Two of them encoded N-truncated MSP58 proteins, lacking 120 and 210 amino acids, and one encoded a C-truncated mutant lacking 182 amino acids. We co-transfected these constructs with the STRA13/FLAG construct in 293T cells and 48 h post-transfection performed co-immunoprecipitation as described above. We found that deletion of the MSP58 C terminus, which contains an FHA domain, resulted in binding abrogation, while deletion of a substantial area of the N terminus did not prevent binding of MSP58 to the STRA13 protein (fig. 2D). These data suggest that the FHA domain of MSP58 is responsible for the interaction with STRA13.

Co-expression of MSP58 and STRA13 increases stability of both MSP58 and STRA13 proteins

Co-expression of MSP58 and the full-length STRA13 protein in 293T cells always resulted in a higher amount of MSP58 in these cells compared to cells co-expressing MSP58 and STRA13 deletion mutants (data not shown). To study the effect of STRA13 and pMSP58 stabilization in more detail, we transiently co-transfected 293T cells with the MSP58/HA construct and each of the following: the full-length STRA13/FLAG construct, a C-truncated 1–299 STRA13 construct, or empty plasmid. Forty-eight hours after transfection, cells were solubilized and analyzed by SDS-PAGE and Western blotting with an anti-HA antibody. In the absence of the exogenously expressed STRA13 or in the combination with the 1–299 mutant, the amount of the MSP58/HA protein was low. In contrast, an approximately fourfold increase in the MSP58 protein level was observed upon its co-expression with the full-length STRA13/FLAG protein (fig. 3A). Thus, taking into consideration our data on MSP58 and STRA13 interacting domains, we can conclude that binding to full-length STRA13 leads to stabilization of the MSP58 protein while binding to the C-truncated STRA13 mutant does not affect MSP58 stability.

Experiments on co-expression of the full-length STRA13 and the MSP58 deletion mutants in 293T cells demonstrated that deletion of the C-terminal part of the MSP58 protein abrogated the stabilizing effect of the STRA13 protein (fig. 3B). These data are in line with the mapping of the STRA13 and MSP58 interaction domains indicating that binding to STRA13 is crucial for MSP58 stabilization.

To further confirm the effect of STRA13 on MSP58 stabilization, we applied cycloheximide to cells co-transfected with STRA13 and MSP58. The MSP58 half-life increased from ~2 h in cells expressing the protein alone to ~8 h in cells expressing both STRA13 and MSP58 (fig. 3C).

In a similar fashion, we checked whether the STRA13 protein half-life is also increased upon MSP58/STRA13 co-expression. Experiments with cycloheximide treatment showed that the STRA13 protein half-life was increased about twofold upon co-expression with MSP58 (fig. 3D). Taken together, these results suggest that binding of STRA13 to MSP58 inhibits degradation of both proteins.

Inhibition of 26S proteasome activity leads to accumulation of MSP58

We showed previously that STRA13 is regulated via the ubiquitin-dependent 26S proteasome pathway [2]. An increase in MSP58 stability observed upon co-expression with the full-length STRA13 protein raised the question about the protein degradation pathway used for MSP58 proteolysis. To identify this pathway, we transfected 293T cells with the MSP58/HA expression vector and exposed the cells to various concentrations of the proteasome inhibitor ALLnL, a cysteine proteinase inhibitor E-64, and a membrane-permeable inhibitor of thiol proteases E-64d (cathepsin B/H/L and calpain). The last two inhibitors were applied to block the lysosome degradation pathway. Treatment of transfected cells with ALLnL resulted in the accumulation of MSP58 in a dose-dependent manner (fig. 4A). Inhibitors of the lysosome degradation pathway, in contrast, did not produce any effect on the MSP58 protein level (fig. 4A). Treatment of the cells with vehicle alone (Me_2SO) also did not produce any change (not shown). These data clearly demonstrate that the level of pMSP58 in the cells is regulated through the 26S proteasome degradation pathway.

The amount of MSP58 in ALLnL-treated cells co-expressing MSP58 and an empty vector was approximately the same as in nontreated cells that co-expressed MSP58 and STRA13 (fig. 4B). Thus, ALLnL treatment of the cells co-expressing both proteins does not add much to the MSP58/STRA13 stabilization, indicating that proteolysis is already inhibited. Interestingly, accumulation of presumably ubiquitinated high-molecular complexes (shown in fig. 4B with brackets) was noticeable not only after proteasome inhibition but also upon co-expression of both proteins. Taken together, these and the above data suggest that the MSP58/STRA13 interaction protects both proteins from the 26S proteasome degradation machinery.

Phosphorylation modulates MSP58/STRA13 interaction

FHA domains may bind phosphothreonine, phosphoserine, and sometimes phosphotyrosine, distinguishing

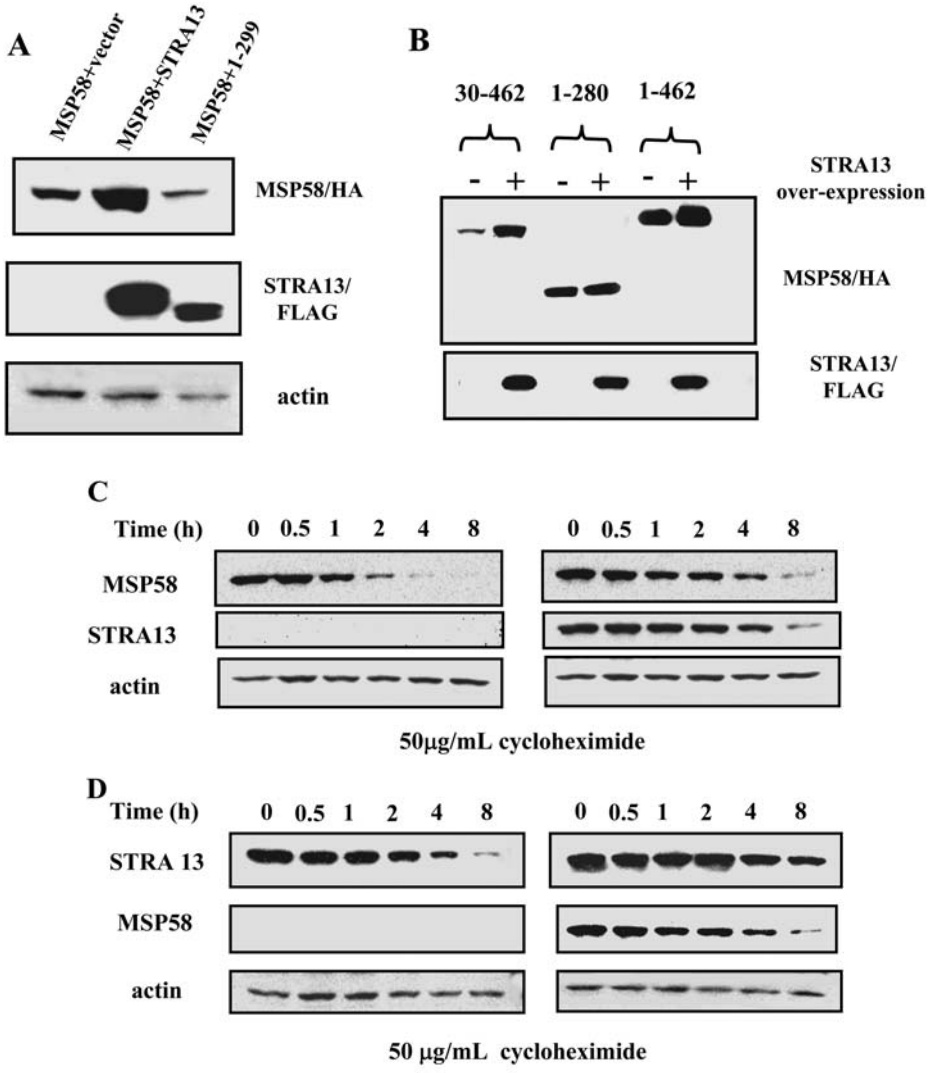

Figure 3. Interaction of MSP58 and STRA13 leads to stabilization of both proteins. (*A*) STRA13/MSP58 co-expression leads to an increase in the MSP58 protein level. 293T cells were transiently co-transfected with MSP58-HA and STRA13-FLAG, STRA13 mutant (1–299), or empty pCMV2 plasmid as a control. The protein level of MSP58 was determined by Western blot with anti-HA rat antibodies. (*B*) Mapping of the MSP58 protein domain responsible for stabilization of MSP58 upon binding to STRA13. 293T cells were transiently co-transfected with MSP58-HA, its mutants and with STRA13 or the pCMV2 empty plasmids. The protein levels of MSP58 and its mutants were determined by Western blot with anti-HA rat antibodies. (*C*, *D*) Co-expression of STRA13 and MSP58 increases the MSP58 level (*C*) and STRA13 protein half-life (*D*). The amount of STRA13 or MSP58 at the indicated time points following the addition of 50 μg/ml cycloheximide was analyzed with anti-FLAG M2 antibodies or anti-HA antibodies, respectively. Even loading on the lanes was ensured by measuring total protein concentration. The half-life was calculated as the mean of two independent experiments.

these domains from other well-studied phosphoprotein-binding domains [23]. Since the MSP58 protein possesses a well-defined C-terminal FHA domain, we designed a set of experiments to determine whether the interaction between STRA13 and MSP58 could be modulated by phosphorylation. To enrich the pool of phosphorylated proteins, we treated cells with sodium pervanadate (PV), a commonly used protein-tyrosine phosphatase inhibitor [24], or with calyculin A, a serine/threonine phosphatase inhibitor (Cell Signaling). A 30-min treatment of 293T cells transiently transfected with the STRA13-FLAG and MSP58-HA constructs significantly increased the amount of the MSP58-HA protein immunoprecipitated with anti-FLAG (STRA13) antibodies as compared to untreated cells (fig. 5A) suggesting that binding of MSP58 to STRA13 may be modulated by the phosphorylation status of these proteins.

Since there are no data available so far on the phosphorylation of these two proteins, we assessed their phosphorylation patterns using a set of STRA13 and MSP58 deletion constructs. 293T cells were transfected with either the full-length STRA13/FLAG construct or each of the following mutants: two N-terminal (259–412, 293–412) mutants, one C-terminal (1–299) mutant, and one mutant

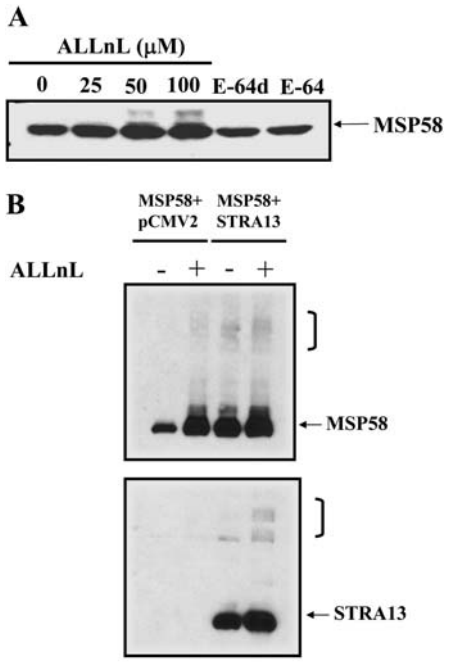

Figure 4. MSP58 is subject to 26S proteasome degradation. (*A*) The proteasome inhibitor ALLnL but not lysosome inhibitors E-64 and E-64d block degradation of MSP58. 293T cells transiently transfected with the MSP58/HA plasmid were treated for 18 h with various concentrations of ALLnL, E-64, and E-64d. Vehicle alone (DMSO) was added to the control plate (*B*) MSP58 protein level at its near maximum upon co-expression with the STRA13 protein. 293T cells transfected either with MSP58/HA and either empty pCMV2 plasmid or STRA13/FLAG construct were treated with 100 μM ALLnL. DMSO-treated cells were used as a control.

lacking both termini of the STRA13 protein (123–299). Thirty-six hours post-transfection, the cells were treated with calyculin A for 30 min. Inhibition of serine/threonine phosphatases led to the accumulation of lower-mobility forms of the full-length STRA13 protein suggesting a post-translational modification of the protein (fig. 5B, right upper panel). Immunoprecipitation of the protein with anti-FLAG antibodies and Western blot analysis with antibodies against phospho-serine/threonine showed that STRA13 was phosphorylated on serine and (or) threonine. Deletion of the C terminus (mutant 1–299) or a large part of the N terminus (mutant 259–412) of the STRA13 protein did not abrogate the phosphorylation on serine/threonine residues (fig. 5B, right upper panel). The mutant lacking both C and N termini (mutant 123–299) also retained its ability for phosphorylation on serine and (or) threonine. However, more extensive deletion of the N terminus (mutant 293–412) eliminated this type of phosphorylation. These results are consistent with the predicted localization of the phosphorylation sites (NetPhos 2.0 Server, http://www.cbs.dtu. dk/services/NetPhos/) in the STRA13 protein. Figure 5C shows that most of the high-score serine and threonine phosphorylation sites are localized within the N-terminal 300 amino acids of the STRA13 protein. The fact that the rest of the protein (residues 300–412) does not possess any serine, threonine phosphorylation sites was confirmed experimentally (fig. 5B, right upper panel).

PV treatment of the transfected cells described above did not result in any visible shift to the lower-mobility forms of the STRA13 proteins. However, immunoprecipitation with anti-FLAG antibodies followed by Western blot analysis with anti-phosphotyrosine antibodies revealed that the STRA13 protein and its mutants were highly and stably phosphorylated on tyrosine even without phosphatase inhibitor treatment. The existence of the STRA13 predominantly in the tyrosine-phosphorylated form may fully account for the observed lack of PV effect. There are two predicted tyrosine phoshorylation sites in the STRA13 protein positioned near its N and C termini (fig. 5C). The fact that the full-length protein was much more phosphorylated on tyrosine than any of the STRA13 mutants lacking the N or C termini (fig. 5B, right lower panel) suggested that both tyrosine phoshorylation sites are functional. Deletion of both STRA13 termini that contain predicted sites of tyrosine phosphorylation resulted in complete abrogation of phosphorylation, implying that only Y^{53} and Y^{335} residues are involved in the tyrosine phosphorylation of the STRA13 protein.

In our MSP58 protein phosphorylation study, we used three deletion mutants of MSP58 that lacked N or C termini: 30–462, 121–462 and 1–280. We demonstrated that the MSP58 protein, as well as its two mutants, 30–462 and 1–280, were capable of phosphorylation on serine/threonine residues (fig. 5B, left upper panel), while the 121–462 mutant did not show any shift in electrophoretic mobility and was not phosphorylated on serine or threonine. These data suggest that all functional serine/threonine phosphorylation sites are localized in the first 120 N-terminal residues of the MSP58 protein.

No tyrosine phosphorylation of the MSP58 proteins was revealed in our assay (fig. 5B, left lower panel) despite the presence of a high-score tyrosine phosphorylation site at position 413 (fig. 5C).

Both MSP58 and STRA13 are regulated in a cell cycle-dependent manner

MSP58 protein accumulation was previously shown to be cell cycle dependent [20]. In this study, we assessed how expression levels of both MSP58 and STRA13 depend on the cell cycle. Growth of 293T cells was blocked at the G1/S interphase (see Materials and methods), and the cells were harvested at different time intervals after release from the block. Equal amounts of RNA isolated from these cells were used for quantitative RT-PCR with primers specific for the coding regions of MSP58 and STRA13. As shown in figure 6A, MSP58 expression was highest at 0.5 h after the release from the block, consistent with the previous report on MSP58 protein cell cycle-de-

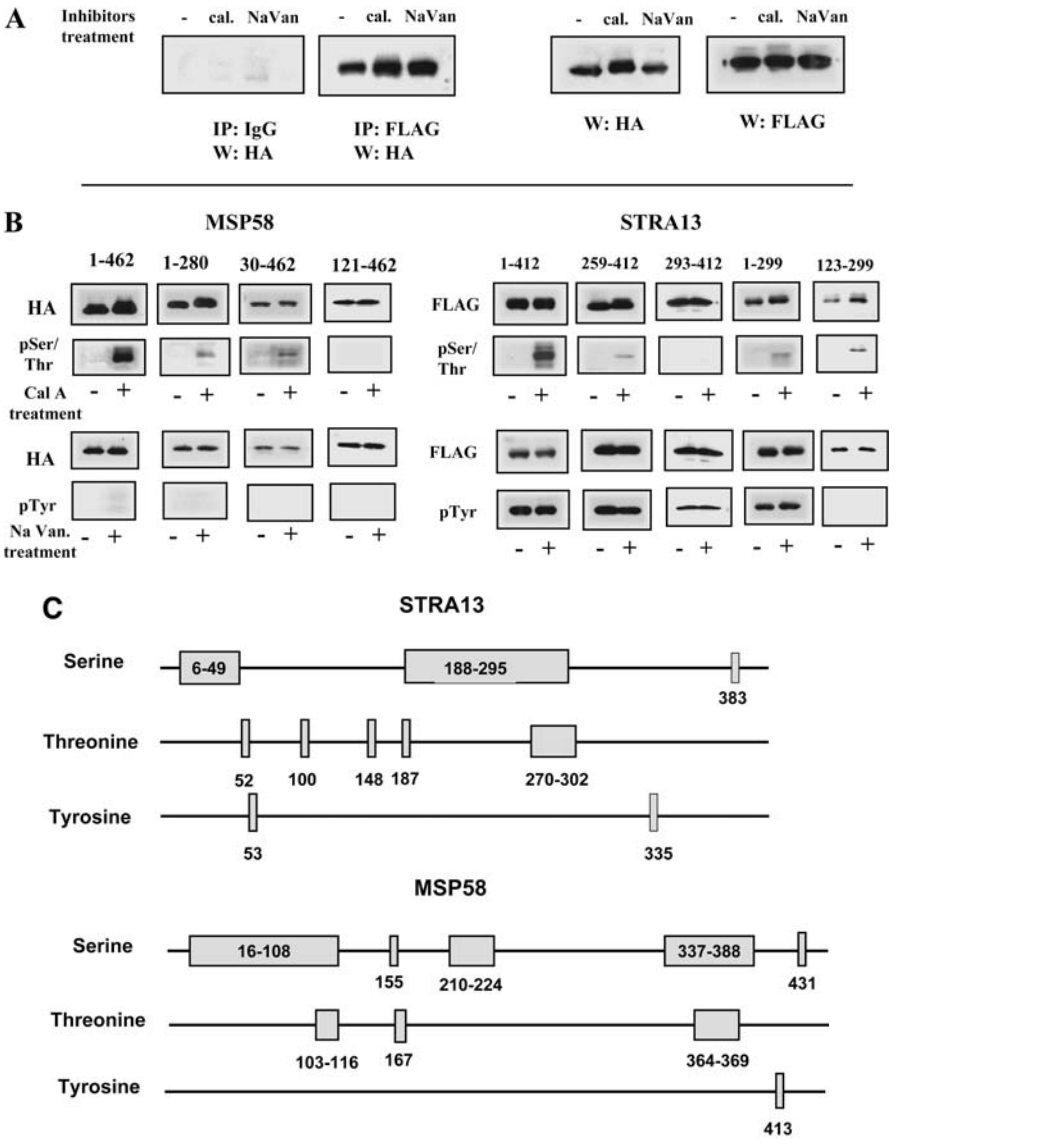

Figure 5. The STRA13/MSP58 interaction is modulated by the phosphorylation status of the STRA13 protein. (*A*) Amount of MSP58/HA immunoprecipitated with STRA13/FLAG is increased by inhibition of phosphatases. STRA13 was immunoprecipitated from cell lysates with anti-FLAG (STRA13) antibodies. Associated MSP58 proteins were detected with anti-HA antibodies. Mouse IgG was used as a control. (*B*) MSP58 is phosphorylated on serine and (or) threonine and not phosphorylated on tyrosine (left panel); STRA13 is phosphorylated on serine, threonine, and on tyrosine (right panel). 293T cells were transfected with the indicated constructs, replated, and treated with the inhibitors as described in Materials and methods. A shift in electrophoretic mobility was analyzed by Western blot analysis with anti-FLAG M2 antibodies for STRA13 protein and its mutants, and with anti-HA antibodies for MSP58 and its mutants. The phosphorylation status of the proteins was determined after immunoprecipitation with the corresponding antibodies and Western blot analysis with rabbit anti-phospho-serine/threonine antibodies or mouse anti-phospho-tyrosine antibodies (Cell Signaling). (*C*) Localization of the predicted high-score phosphorylation sites in the STRA13 and MSP58 protein sequences. The analysis was done using NetPhos 2.0 Server.

pendent accumulation [20]. Based on the RT-PCR evaluation, we also concluded that at least two alternatively spliced isoforms of MSP58 were accumulated during the period of 0.5–3 h after the release from the block. These data suggest that the alternative splicing of MSP58, which we assessed in detail above, is a cell cycle-specific process. Overall, the MSP58 transcript achieved its highest level in the very early S phase stage and was at its lowest in G2, i.e., 7 h after the release from the block. While accumulation of STRA13 mRNA after the release from the block also reached its maximum in the early S phase, it was not as drastically down-regulated as MSP58 afterwards. These data indicate that expression of both STRA13 and MSP58 genes is cell cycle dependent, with similar patterns of expression during the cell cycle.

STRA13 and MSP58 are co-expressed in the nucleus

To determine whether MSP58 co-localizes with STRA13 in the nucleus, expression constructs for HA-tagged MSP58 and FLAG-tagged STRA13 were transfected into 293T cells. Thirty hours post-transfection, the cells were stained with anti-HA and anti-FLAG antibodies and visualized with Alexa Fluor 488- and Alexa Fluor TM 594-conjugated secondary antibodies, respectively (fig. 6B). In the previous studies, exogenously expressed STRA13 was found to be localized predominantly in the nucleus [2, 6]. MSP58 was reported to be mostly of nuclear or nucleolar localization depending on the cell type [18, 19]. Our present study shows that in 293T cells, both MSP58 and STRA13 are confined and co-localized predominantly to the nucleus (fig. 6B, bottom panel, bottom raw). In addition, approximately 15% of cells over-expressing MSP58 displayed other than nuclear localization, such as nucleolar, subnuclear, cytoplasmic, or nuclear/cytoplasmic (fig. 6B, upper panel). STRA13 was restricted to the nucleus independently of MSP58 localization (fig. 6B, bottom panel). Based on these observations, we conclude that STRA13 and MSP58 overlap in subcellular localization, and co-expression of STRA13 and MSP58 does not cause cellular redistribution of these proteins.

Roles of STRA13 and MSP58 in the regulation of STRA13 transcription

Both STRA13 and MSP58 proteins were previously implicated in transcriptional regulation [5, 11, 13, 17, 19]. STRA13 protein was shown to be capable of auto-regulation at the transcriptional level [8]. To determine possible involvement of MSP58 in regulation of the STRA13 promoter, we created a STRA13-Luc reporter construct where a ~1.1-kb region of the STRA13 promoter was in-

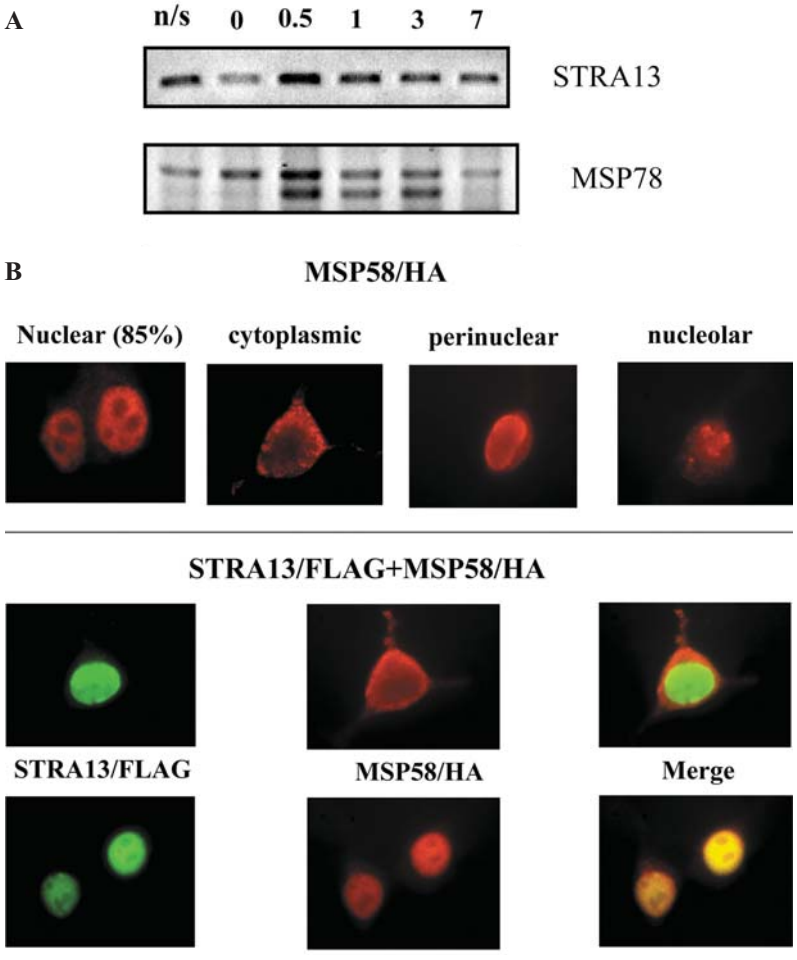

Figure 6. Expression and localization of MSP58 and STRA13 overlap. (*A*) Expression of STRA13 and MSP58 genes is cell cycle dependent. 293T cell total RNA was prepared from unsynchronized (leftmost lane) and synchronized cells at 0, 0.5, 1, 3 and 7 h after release from the double-thymidine block, and RT-PCR was performed as described in Materials and methods. RT-PCR with primers for 18S RNA served as a control. (*B*) Co-localization of the STRA13 and MSP58 proteins in the nucleus. Transfected and fixed cells were immunostained with anti-FLAG monoclonal antibody and anti-HA monoclonal antibody and visualized with anti-mouse Alexa Fluor 488 (green) for the anti-FLAG monoclonal antibody and anti-rat with Alexa Fluor TM 594 (red) antibodies for anti-HA monoclonal antibody. Merged images are also shown.

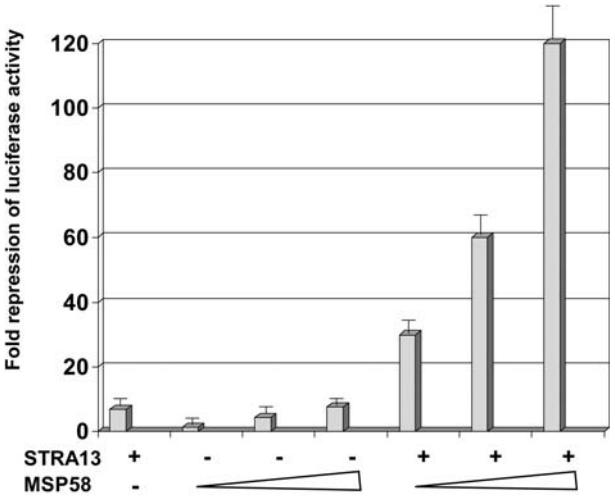

Figure 7. The STRA13/MSP58 complex has a synergistic repression effect on the STRA13 promoter. 293T cells were transiently co-transfected with the STRA13-luciferase construct and the STRA13/FLAG or (and) MSP58/HA constructs in increasing concentrations (1, 2, and 4 µg) where indicated. Fold repression was calculated in comparison with the basal luciferase activity obtained with the pCMV2 vector. The experiments were repeated at least three times. Error bars indicate the SD of mean values.

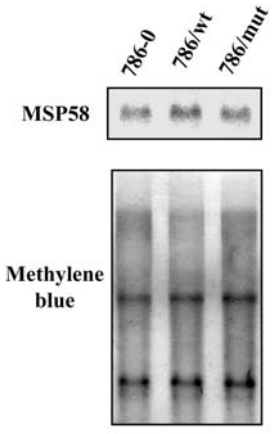

Figure 8. Expression of MSP58 is not under pVHL control. VHL-deficient (786-0, mut) and VHL-proficient (wt) renal clear-cell carcinoma cell lines were analyzed by Northern blot analysis for expression of MSP58. Pre-staining of the membrane with methylene blue shows equal lane loadings.

serted in a luciferase reporter plasmid. Forced expression of STRA13 led to a seven- to tenfold decrease in the STRA13 promoter-driven reporter activity in a STRA13 dosage-dependent manner (fig. 7). MSP58 over-expression also resulted in promoter repression although to a lesser extent (fig. 7). Co-expression of both proteins led to a dramatic suppression of the STRA-luc basal transcription to up to 120 times in a MSP58 dosage-dependent manner (fig. 7). These results imply that the STRA13/MSP58 complex has a synergistic repression effect on the STRA13 promoter.

Expression of the MSP58 transcript is not under pVHL control

STRA13 was identified in our laboratory as a novel hypoxia-inducible pVHL target regulated at the mRNA level [1, 2]. In the present paper, we show that MSP58 may serve as a regulator of STRA13 transcription. To find out whether MSP58 is a pVHL target that could mediate the VHL suppression effect on STRA13, we assessed MSP58 expression levels in VHL-deficient (786-0, mut) and VHL-proficient (wt) renal clear-cell carcinoma cell lines [1]. Northern blot analysis of these cell lines demonstrated that VHL does not play any significant role in the MSP58 regulation since all three cell lines showed the same levels of MSP58 expression (fig. 8).

Discussion

Our study provides biochemical and functional evidence of association between the bHLH transcription factor STRA13 and the cell cycle-dependent transcriptional regulator MSP58. We demonstrate that binding of STRA13 to MSP58 requires their basic and FHA domains, respectively. Although several STRA13 protein partners were characterized recently, the basic domain (pos. 1–67) has not been reported to play a critical role in those interactions. Thus, associations of STRA13 with HDAC1, Sin3A, NCoR, and USF occurs primarily via the large C-terminal region of STRA13 that contains α-helical structures (pos. 128–411), though the interaction with NCoR requires also the intact STRA13 bHLH domain (pos. 1–127) [8, 17]. Binding of STRA13 to Bmal1, a bHLH-PAS transcription factor involved in mammalian molecular clock regulation, utilizes the integral STRA13 bHLH domain [13], while interaction with the STAT3 transcriptional factor employs the bHLH and the short C-terminal (pos. 300–412) domains [5], and association with hUBC9 requires the short C-terminal domain alone [2].

The basic region of bHLH proteins is generally considered to mediate DNA binding, whereas the HLH domain is required for protein dimerization [25]. However, there are a few studies that implicate the basic domain of bHLH in protein-protein interactions. Thus, the bHLH protein USF binds to STRA13 via the USF basic region [17]. Similarly, association of both USF and transcription factor Ets-1 is mediated through their basic domains [26]. USF and Ets-1 synergize in DNA binding as well as in the transactivation of reporter constructs. Interestingly, MSP58 and STRA13 also synergized in their transcriptional repression activity in our reporter assay.

We identified the C-terminal FHA domain of MSP58 as responsible for the MSP58/STRA13 interaction. The FHA domain is a phosphopeptide-binding module first identified in a group of forkhead transcription factors. In yeast and human, many FHA-containing proteins are found in the nucleus where they take part in DNA repair, cell cycle arrest, or pre-mRNA processing. One intriguing finding is that FHA domains may bind phospho-threonine, phospho-serine and sometimes phospho-tyrosine [23].

In our work, we demonstrated that STRA13/MSP58 binding is modulated by phosphorylation. Two functional tyrosine phosphorylation sites were revealed in the STRA13 protein at residues 53 and 335 (fig. 5B, C). Given that the FHA domain of MSP58 binds the basic domain of the STRA13 protein (residues 1–67) that contains Tyr^{53} and that no MSP58 tyrosine phosphorylation was detected, one may suggest a crucial role for the Tyr^{53} residue in modulation of these protein interactions. As for serine/threonine phosphorylation, our phospho-mapping assay associated the 300 N-terminal amino acids of STRA13 and 120 N-terminal residues of MSP58 with this type of phosphorylation. These data rule out the involvement of the FHA domain (residues 355–444) in the modulation of the protein association by phosphorylation. Hence, only tyrosine or serine/threonine phosphorylation of the STRA13 basic domain may be responsible for the binding modulation.

Overall, our data on the association of tyrosine Tyr^{53} or the serine/threonine-phosphorylated basic domain of STRA13 with the FHA domain of MSP58 are in line with the described unique ability of the FHA domain to bind phospho-tyrosine, phospho-threonine, and phospho-serine residues [23].

Here, we report that the amount of MSP58 protein was significantly increased upon co-expression with the full-length STRA13 protein, suggesting stabilization of the MSP58 protein. We found that the basic domain of STRA13 responsible for the interaction with MSP58 is also required for an increase in MSP58 level, implying that binding to STRA13 is a precondition for the MSP58 stabilization. However, lack of MSP58 stabilization upon binding to the STRA13 C-terminal-truncated 1–299 mutant indicates that binding to the basic domain is a necessary but not sufficient step in the process of stabilization of the MSP58 protein. Thus, stabilization of MSP58 by STRA13 requires an essentially intact STRA13 molecule. A C-truncated derivative of MSP58 (1–280 amino acids) that lacks the STRA13-interacting FHA domain was also not accumulated upon co-expression with STRA13, strengthening our conclusion on the stabilizing role of the complex.

The expression level of many transcription factors is controlled by the ubiquitin/26S proteasome system. We showed previously that the STRA13 protein level was controlled by the ubiquitin-dependent proteolysis [2]. Interaction with the ubiquitin-conjugating enzyme hUBC9, a constituent of the proteasome degradation pathway, shortened the STRA13 half-life fourfold [2]. In this paper, we demonstrate, for the first time, that MSP58 is also a subject to the 26S proteasome degradation. In line with our data on STRA13/MSP58 mutual stabilization, treatment of cells co-expressing both STRA13 and MSP58 with proteasome inhibitors did not lead to a significant increase in MSP58 or STRA13 levels as compared to the untreated cells, indicating that the STRA13/MSP58 complex is protected from the 26S proteasome machinery. The observed inhibition of the degradation via the STRA13/MSP58 association may occur at any of the several steps of the proteolytic pathway: (i) ubiquitination of MSP58 and (or) STRA13, (ii) dissociation of the ubiquitinated proteins from the STRA13/MSP58 complex, and (iii) degradation of the ubiquitinated MSP58 and the STRA13 by the proteasome. Accumulation of presumably ubiquitinated large-molecular complexes during MSP58/STRA13 co-expression (fig. 4B) suggests either blocking of the dissociation of the ubiquitinated forms, and/or an impaired degradation of the ubiquitinated MSP58 and STRA13 by the 26S proteasome.

The precise mechanism by which the STRA13/MSP58 complex is stabilized remains to be defined. In the MSP58 case, masking of a PEST sequence (hydrophilic stretches rich in Pro, Glu/Asp, Ser, and Thr) that is required for the degradation of certain Ub-dependent substrates [27] may be involved. Analysis of the MSP58 protein sequence using the PESTfind server (www.at.embnet.org/embnet/tools/bio/PESTfind/about.htm) revealed one putative PEST region at positions 82–93 with a high PESTfind score of +10.7, (range of –50 to +50, threshold >+5), while no statistically significant PEST regions were found in the STRA13 protein. In turn, MSP58 may inhibit STRA13 degradation by blocking the STRA13 C-terminal region that was previously shown by us to be crucial for hUBC9 binding [2] and the subsequent degradation via ubiquitin-mediated proteolysis.

Thus, we have shown that one important function of the STRA13 and MSP58 association is to stabilize both proteins protecting them from the 26S proteasome degradation. Immunofluorescent staining of 293T cells co-expressing STRA13 and MSP58 revealed no distinctive sub-cellular compartmentalization of the complex upon co-expression of the proteins. These data are in line with our hypothesis on STRA13/MSP58 stabilization through masking of protein-degradation signals making sequestration of the complex to a special ‘proteasome machinery-proof’ cellular compartment less feasible.

A similar protein stabilization mechanism was demonstrated for two yeast transcription factors, MATα1 and MATα2. Both were stabilized by heterodimerization that prevented degradation by masking the ubiquitin recogni-

tion signal [28]. Another example of such mutual stabilization is the prevention of proteasome-dependent degradation of the VHL protein by the elongin BC complex [29].

Since complex formation between STRA13 and MSP58 results in mutual stabilization, the putative function of the complex is most likely to potentiate activity of STRA13 or MSP58 (or both) rather than down-regulate them. We tested this hypothesis by studying the effect of co-expression of these transcriptional factors on transcription of a target gene. Co-expression of STRA13 and MSP58 in 293T cells resulted in a dramatic synergistic suppression of the STRA13 promoter in an MSP58 concentration-dependent manner, thus confirming our potentiation hypothesis. These results taken together with the data on the stabilization of the MSP58/STRA13 complex strongly suggest that MSP58 and STRA13 form a durable and effective repression complex in the nucleus.

In our previous work, we described STRA13 as a pVHL target whose expression was down-regulated by pVHL at the mRNA level [2]. In the present study, we show that MSP58 may repress the STRA13-luciferase promoter, implying the existence of an MSP58-dependent regulation of the endogenous level of STRA13 mRNA. In a next step, we checked whether the MSP58 transcript can be up-regulated by pVHL mediating the VHL suppression effect on STRA13. Northern blot analysis did not support pVHL involvement in MSP58 transcriptional control. Therefore, we conclude that MSP58 regulation is unlikely to be directly linked to the VHL/HIF-dependent pathway, and more studies are needed to better understand the mechanisms of regulation of MSP58 expression.

In conclusion, identification and characterization of a new STRA13 protein partner, MSP58, opens a new perspective on the association of STRA13 activity with cell cycle regulation. Both STRA13 and MSP58 were implicated in the regulation of proliferation and apoptosis. Association of these proteins results in a robust transcriptional repressor complex protected from protein degradation. Co-expression of both proteins in early S phase is especially intriguing in the context of HIF1α involvement in rapid hypoxia-induced replication arrest and apoptosis, which was documented recently in a number of studies [30–32]. Characterization of STRA13/MSP58 transcriptional targets will provide more insight into hypoxia-associated growth regulation and its relevance to carcinogenesis.

Acknowledgements. This project was funded in whole or in part with Federal funds from the National Cancer Institute, National Institutes of Health, and Contract No. NO1-CO-56000 (A. I., S. I.). The content of the publication does not necessarily reflect the views or policies of the Department of Health and Human Services, nor does mention of trade names, commercial products, or organizations imply endorsement by the U.S. Government.

References

1 Ivanov S. V., Kuzmin I., Wei M. H., Pack S., Geil L., Johnson B. E. et.al. (1998) Down-regulation of transmembrane carbonic anhydrases in renal cell carcinoma cell lines by wild-type von Hippel-Lindau transgenes. Proc. Natl. Acad. Sci. USA **95:** 12596–12601

2 Ivanova A. V., Ivanov S. V., Danilkovitch-Miagkova A. and Lerman M. I. (2001) Regulation of STRA13 by the von Hippel-Lindau tumor suppressor protein, hypoxia, and the UBC9/ubiquitin proteasome degradation pathway. J. Biol. Chem. **276:** 15306–15315

3 Miyazaki K., Kawamoto T., Tanimoto K., Nishiyama M., Honda H. and Kato Y. (2002) Identification of functional hypoxia response elements in the promoter region of the DEC1 and DEC2 genes. J. Biol. Chem. **49:** 47014–47021

4 Zawel L., Yu J., Torrance C. J., Markowitz S., Kinzler K. W., Vogelstein B. et al. (2002) DEC1 is a downstream target of TGF-beta with sequence-specific transcriptional repressor activities. Proc. Natl. Acad. Sci. USA **99:** 2848–2853

5 Ivanova A. V., Ivanov S. V., Zhang X., Ivanov V. N., Timofeeva O. A. and Lerman M. I. (2004) STRA13 interacts with STAT3 and modulates transcription of STAT3-dependent targets. J. Mol. Biol. **340:** 641–653

6 Boudjelal M., Taneja R., Matsubara S., Bouillet P., Dolle P. and Chambon P. (1997) Overexpression of Stra13, a novel retinoic acid-inducible gene of the basic helix-loop-helix family, inhibits mesodermal and promotes neuronal differentiation of P19 cells. Genes Dev. **16:** 2052–2065

7 Shen M., Kawamoto T., Teramoto M., Makihira S., Fujimoto K., Yan W. et. al. (2001) Induction of basic helix-loop-helix protein DEC1 (BHLHB2)/Stra13/Sharp2 in response to the cyclic adenosine monophosphate pathway. Eur. J. Cell Biol. **80:** 329–334

8 Sun H. and Taneja R. (2000) Stra13 expression is associated with growth arrest and represses transcription through histone deacetylase (HDAC)-dependent and HDAC-independent mechanisms. Proc. Natl. Acad. Sci. USA **8:** 4058–4063

9 Yamada K., Kawata H., Mizutani T., Arima T., Yazawa T., Matsuura K. et al. (2004) Gene expression of basic helix-loop-helix transcription factor, SHARP-2, is regulated by gonadotropins in the rat ovary and MA-10 cells. Biol. Reprod. **70:** 76–82

10 Yamada K., Kawata H., Shou Z., Mizutani T., Noguchi T. and Miyamoto K. (2003) Insulin induces the expression of the SHARP-2/Stra13/DEC1 gene via a phosphoinositide 3-kinase pathway. J. Biol. Chem. **33:** 30719–30724

11 Yun Z., Maecker H. L., Johnson R. S. and Giaccia A. J. (2002) Inhibition of PPARgamma2 gene expression by the HIF-1-regulated gene DEC1/Stra13: a mechanism for regulation of adipogenesis by hypoxia. Dev. Cell. **2:** 331–341

12 Shen M., Yoshida E., Yan W., Kawamoto T., Suardita K., Koyano Y. et. al. (2002) Basic helix-loop-helix protein DEC1 promotes chondrocyte differentiation at the early and terminal stages. J. Biol. Chem. **277:** 50112–50120

13 Honma S., Kawamoto T., Takagi Y., Fujimoto K., Sato F., Noshiro M. et al. (2002) DEC1 and DEC2 are regulators of the mammalian molecular clock. Nature **419:** 841–844

14 Grechez-Cassiau A., Panda S., Lacoche S., Teboul M., Azmi S., Laudet V. et al. (2004) The transcriptional repressor STRA13 regulates a subset of peripheral circadian outputs. J. Biol. Chem. **279:** 1141–1150

15 Sun H., Lu B., Li R. Q., Flavell R. A. and Taneja R. (2001) Defective T cell activation and autoimmune disorder in Stra13-deficient mice. Nat. Immunol. **2:** 1040–1047

16 Seimiya M., Wada A., Kawamura K., Sakamoto A., Ohkubo Y., Okada S. et. al. **(**2004) Impaired lymphocyte development and function in Clast5/Stra13/DEC1-transgenic mice. Eur. J. Immunol. **34:** 1322–1332

17 Dhar M. and Taneja R. (2001) Cross-regulatory interaction between Stra13 and USF results in functional antagonism. Oncogene **20:** 4750–4756
18 Ren Y., Busch R. K., Perlaky L. and Busch H. (1998) The 58-kDa microspherule protein (MSP58), a nucleolar protein, interacts with nucleolar protein p120. Eur. J. Biochem. **253:** 734–742
19 Lin D. Y. and Shih H. M. (2002) Essential role of the 58-kDa microspherule protein in the modulation of daxx-dependent transcriptional repression as revealed by nucleolar sequestration. J. Biol. Chem. **277:** 25446–25456
20 Bruni R. and Roizman B. (1998) Herpes simplex virus 1 regulatory protein ICP22 interacts with a new cell cycle-regulated factor and accumulates in a cell cycle-dependent fashion in infected cells. J. Virol. **72:** 8525–8531
21 Bader A. G., Schneider M. L., Bister K. and Hartl M. (2001) TOJ3, a target of the v-Jun transcription factor, encodes a protein with transforming activity related to human microspherule protein 1 (MCRS1). Oncogene **20:** 7524–7535
22 Song H., Li Y., Chen G., Xing Z., Zhao J., Yokoyama K. K. et al. (2004) Human MCRS2, a cell-cycle-dependent protein, associates with LPTS/PinX1 and reduces the telomere length. Biochem. Biophys. Res. Commun. **316:** 1116–1123
23 Li J., Lee G. I., Van Doren S. R. and Walker J. C. (2000) The FHA domain mediates phosphoprotein interactions. J. Cell Sci. **113:** 4143–4149
24 Gordon J. A. (1991) Use of vanadate as protein-phosphotyrosine phosphatase inhibitor. Methods Enzymol. **201:** 477–482
25 Davis R. L. and Turner D. L. (2001) Vertebrate hairy and enhancer of split related proteins: transcriptional repressors regulating cellular differentiation and embryonic patterning. Oncogene **20:** 8342–8357
26 Sieweke M. H., Tekotte H., Jarosch U. and Graf T. (1998) Cooperative interaction of ets-1 with USF-1 required for HIV-1 enhancer activity in T cells. EMBO J. **17:** 1728–1739
27 Rechsteiner M. and Rogers S. W. (1996) PEST sequences and regulation by proteolysis. Trends Biochem. Sci. **21:** 267–271
28 Johnson P. R., Swanson R., Rakhilina L. and Hochstrasser M. (1998) Degradation signal masking by heterodimerization of MATalpha2 and MATa1 blocks their mutual destruction by the ubiquitin-proteasome pathway. Cell **94:** 217–227
29 Schoenfeld A. R., Davidowitz E. J. and Burk R. D. (2000) Elongin BC complex prevents degradation of von Hippel-Lindau tumor suppressor gene products. Proc. Natl. Acad. Sci. USA **97:** 8507–8512
30 Gardner L. B., Li Q., Park M. S., Flanagan W. M., Semenza G. L. and Dang C. V. (2001) Hypoxia inhibits G1/S transition through regulation of p27 expression. J. Biol. Chem. **276:** 7919–7926
31 Goda N., Ryan H. E., Khadivi B., McNulty W., Rickert R. C. and Johnson R. S. **(**2003) Hypoxia-inducible factor 1alpha is essential for cell cycle arrest during hypoxia. Mol. Cell. Biol. **23:** 359–369
32 Schmaltz C., Hardenbergh P. H., Wells A. and Fisher D. E. (1998) Regulation of proliferation-survival decisions during tumor cell hypoxia. Mol. Cell. Biol. **18:** 2845–2854